15.6 Quantifying near-surface winds in tornadoes: A combined DOW-LES approach

Karen A. Kosiba* and Robert J. Trapp
Purdue University, West Lafayette, IN

1. Introduction

Although theory, modeling, and observation have provided us with a general framework for understanding tornadic flow, obtaining a comprehensive picture of the low-level wind field remains an ongoing endeavor. The near-surface winds in a tornado are a complex interaction of three dynamically different regions of flow: the swirling boundary layer, the corner region, and the core flow. A simplified view of the interaction between these regions consists of the boundary layer feeding the vortex core by way of the corner region. The boundary layer, which is believed to comprise roughly the lowest 100 meters of flow, forms as a result of the strong interaction of the primary rotating flow with the underlying surface (Davies-Jones et al. 2001). Above the boundary layer, the flow is approximately in cyclostrophic balance and dictates the magnitude of the radial pressure gradient force in the boundary layer. Since frictional interaction necessarily reduces the tangential velocity to zero at the surface, an imbalance is created between the centrifugal and radial pressure gradient forces. This imbalance drives a net inward acceleration, resulting in increased tangential velocities in the mid- to upper- boundary layer.

Flow diverted into the boundary layer and subsequently into the core must pass through the corner region, the most dynamically complex region of the tornado. Unlike other regions of the tornado, all three components of velocity are important in this region. The corner region--a region that has approximately the same vertical extent as the boundary layer and the same horizontal extent as the core--is where the horizontal boundary layer flow must turn vertical. Flow in this region can be additionally complicated by the presence of vortex breakdown, which could result in the largest velocities occurring very close to the ground. Since the vortex core consists of air that has entered either from the flow aloft or from the boundary layer, changes in the boundary layer flow can substantially alter the core flow by way of the corner region. Of particular interest to us is how vertical and temporal variations in the flow immediately surrounding the tornado affect its structure and evolution, and thus the propensity for a tornado to inflict damage.

Results obtained from laboratory and numerical experiments of vortical flow indicate that the swirl ratio ($S = v_0/w_0$, where v_0 is the outer swirl velocity and w_0 is the average vertical velocity) uniquely describes vortex structure. While the swirl ratio is a readily defined quantity in both laboratory and numerical simulations, it can be a rather ambiguous quantity to calculate in actual tornadoes (e.g., Lee and Wurman 2005). Unlike in modeling experiments in which the swirl ratio is a controlled, time-independent quantity, the swirl ratio associated with a tornado is a *time-*

* *Corresponding author address:* Karen A. Kosiba, Purdue University, Dept. of Earth and Atmospheric Sciences, West Lafayette, IN 47907-2051; email: kakosiba@purdue.edu

dependent parameter. Thus tornadic flow may have an associated response period during which the tornado would evolve through different structures and, consequently, varied velocity distributions, while adjusting to the changing swirl ratio. Additionally, in the atmosphere v_0 and w_0 are not constant in height, as typically idealized in modeling studies, further complicating a straightforward analogy between swirl ratio and vortex structure.

All of the aforementioned regions are modulated by turbulent interactions and the outer flow conditions (i.e., the boundary conditions). The details of these turbulent interactions and changes in the outer flow conditions are paramount in establishing tornado-vortex dynamics, and consequently the magnitude and the location of the maximum wind speed. As mentioned above (discussed in the context of the swirl ratio), the outer flow conditions are much more complicated than those used in current numerical models of tornadoes. Not only does the outer flow display significant spatial variation, but it is also rapidly changing in time. This may have implications on the instantaneous vortex structure as well as the velocity distribution within the tornado.

2. Methodology

From both a modeling and an observational perspective, quantifying the low-level winds in a tornado is not a straightforward task. This is due in part to the necessity of representing the turbulent properties of the flow in a numerical model, or to the logistics of collecting data in this most hazardous region.

In order to model the flow at a resolution sufficient to resolve the energy-containing turbulent eddies ($\Delta \sim O$ (10m), where Δ is the grid spacing; e.g., Lewellen et al. 1997), it is not computationally feasible to model the entire environment of the tornado (i.e., the parent thunderstorm). One is thereby forced to make some simplifications or choices on how this information should be relayed to or represented on the tornado-scale grid. In the early 1990's, the large-eddy simulation was employed for tornado-scale research (Lewellen 1993). This approach was shown to be computationally advantageous while still preserving the essential turbulent nature of the flow. Boundary conditions on the model serve to relay the relevant outer flow dynamics to the model grid; hence the appropriate choice of lateral and top boundary conditions is paramount. Thus far, the degree to which boundary conditions have been employed has only allowed for an idealized realization of low-level tornado dynamics.

DOW observations (e.g., Lee and Wurman 2005) suggest that the outer flow of tornadoes is much more complex than the idealized boundary conditions applied in LES models. As a first approach, this disconnect between observation and model is remedied by using DOW-derived 3D winds (which exhibit vertical variability) as the boundary conditions on an LES. While our DOW-LES approach is not without its own simplifications and subsequent limitations, it does allow for the variability present in the outer flow to be manifested in the tornado, thus allowing for the assessment of the realization of idealized constructs in the near-surface winds. This approach both augments DOW observations and builds upon idealized LES models.

a. Doppler Radar Analysis

Two cases appropriate for this research have already been collected by the DOWs: the 30 May 1998 Spencer, SD tornado and the 12 May 2004 Harper, KS tornado. Both of these data sets contain full radar volume scans from near the surface (~ 15-30 m AGL) to several hundred kilometers. As the LES model requires a Cartesian grid, the radar data has been bilinearly interpolated from radar to Cartesian coordinates using NCAR's SPRINT software. For the Harper, KS tornado, a grid spacing of 25 m was chosen to accommodate the varied azimuthal and range resolution of the radar data.

In order to specify the boundary conditions on the LES model, the velocity components (i.e., radial and tangential) of the wind must be obtained from the radar observations. Since the data sets used in this research are single Doppler, the radial (u) and tangential (v) winds need to be retrieved from the measured Doppler velocities. In order to do so, we have elected to utilize the axisymmetric model (Dowell et al. 2005) because it provides a simple, yet robust method for extracting the horizontal winds. Underlying this model is the critical assumption that the tornado and its surrounding flow can be considered a superposition of axisymmetric rotational and divergent flows in conjunction with a background flow. Consequently, this model only retrieves the axisymmetric, or wavenumber 0, components of the flow. Although there is some evidence of core flow asymmetries in the both data sets, the surrounding flow (i.e., the outer core flow) is assumed to be primarily axisymmetric. Unfortunately, introducing asymmetries at this point in the research would be too ambitious, but such dependencies will ultimately be explored in subsequent investigations.

The observed Doppler velocity (D) can then be expressed as follows (eqn.1):

$$D = u\cos(\alpha-\theta) + v\sin(\alpha-\theta) + C\cos(\beta-\theta)$$

where α is the angle of the observation with respect to the tornado center, θ is the angle of the observation with respect to the radar, C is the translational speed of the tornado, and β is the translational angle of the tornado with respect to the tornado center (Fig. 1). In this formulation, the vertical wind component measured by the radar is omitted because the change in height over the area of interest at low elevation angles is relatively small. Solving equation (1) in a least squares sense in an annulus surrounding the vortex center yields the following relations for the azimuthally-averaged (wavenumber 0) radial and tangential winds:

$$u(r) = \frac{\sum_i a_i^2 \sum_i b_i c_i - \sum_i a_i b_i \sum_i a_i c_i}{\sum_i a_i^2 \sum_i b_i^2 - \left(\sum_i a_i b_i\right)^2} \qquad (2)$$

,

$$v(r) = \frac{\sum_i b_i^2 \sum_i a_i c_i - \sum_i a_i b_i \sum_i b_i c_i}{\sum_i a_i^2 \sum_i b_i^2 - \left(\sum_i a_i b_i\right)^2} \qquad (3)$$

where *i* refers to the index of observation along the annulus and

$$\begin{aligned} a_i &= \sin(\alpha_i - \theta_i) \\ b_i &= \cos(\alpha_i - \theta_i) \\ c_i &= D_i - C\cos(\beta - \theta_i) \end{aligned} \qquad (4)$$

The motion (i.e., the speed and direction) of the tornado needs to be calculated *a priori* between successive volume scans. This is accomplished by plotting and then tracking the center of the tornado--defined as the midpoint between the maximum inbound and outbound Doppler velocities--at the 100 m level--throughout the lifetime of the tornado. Each location, then, has a different C and β to be incorporated into the wind retrievals.

The assumption of axisymmetry allows for the horizontal divergence to be calculated from the radial wind component (Lee et al. 2000):

$$\nabla_h \cdot \vec{V} = \frac{\partial u}{\partial r} + \frac{u}{r} \qquad (5)$$

Once the axisymmetric divergence is found, the continuity equation can then be integrated to obtain the axisymmetric vertical wind (w):

$$\rho w = \int_{z(k)}^{z(k+1)} \rho\left(\nabla_h \cdot \vec{V}\right) dz \qquad (6)$$

Other pertinent quantities used to diagnose vortex kinematics, such as vertical vorticity (ζ), circulation (Γ), and angular momentum (M), are derived from the retrieved winds:

$$\zeta = \frac{\partial v}{\partial r} + \frac{v}{r} \qquad (7)$$

$$\Gamma = \oint_C v\, dl \qquad (8)$$

$$M = vr \qquad (9)$$

b. LES

Currently, we are evaluating two different models for use as the LES: the NCAR LES (Moeng 1984) and the Weather Research and Forecasting (WRF) model (Skamarock et al. 2005). Either model requires alteration of the code in order to specify the DOW-derived boundary conditions.

Based on the work of Lewellen at al. (1997), an initial 3D (Cartesian-coordinate) model domain of 1 km × 1 km × 1 km with a grid spacing of Δx = Δy = Δz = 5 m will be employed; further experimentation will determine the optimal choices. Both models allow for the inclusion of a finer mesh within the outer, coarser grid for increased resolution; this option may need to be utilized in the lowest few tens of meters AGL in order to gain a more detailed picture of the near-surface flow. As noted earlier, limited computational resources and the need for relatively small gridpoint spacing, necessarily limit the extent of the model domain. Therefore, the boundary conditions need to accurately preserve the essential characteristics of the larger scale environment.

DOW-derived values of the radial, tangential and vertical winds will provide the lateral and top boundary conditions. The top boundary condition will be specified by the vertical velocity (as a function of radius) derived (from the continuity equation) for the 1 km level. The lateral boundary conditions will be given by the radial and tangential wind components. In the lowest several meters, where radar data does not exist, two approaches will initially be taken: (1) data from the lowest elevation scan will be applied uniformly through this layer and (2) below the lowest elevation scan a logarithmic profile will be specified. This will be done in order to determine which distribution best replicates the winds aloft.

3. DOW analysis of the 12 May 2004 Harper, KS tornado

Initially, from 01:39:00 to 01:41:00 UTC (all times are references to the minute corresponding to the start of the volume scan), there is strong flow (~ 20 m s^{-1}) into the tornado at all radii (Fig. 2). As the tornado evolves, the flow within approximately the radius of maximum winds is notably divergent. Outside of the radius of maximum winds (RMW), there is still flow into the tornado, albeit visibly weaker than at the beginning of the analysis period. This change in the radial velocity within the RMW may be indicative of the transition to a two-celled vortex, which is further elucidated by the development of a downdraft (Fig. 3).

The initial surge of inflow is accompanied by a comparatively large swath of tangential winds in excess of 32 m s^{-1} (the lower bound on F0 winds). After 01:41:00, the tornado contracts, as is evidenced by the decrease in the RMW. After this contraction, the tornado increases in both size and intensity (as measured by the peak tangential winds) so that between 01:50:00 and 01:54:00 (the last time data was available), the tornado was not only at its peak intensity, but additionally, winds in excess of 32 m s^{-1} extended well beyond the RMW (Fig. 4).

Figure 5 depicts the angular momentum at 01:52:00, when the tornado was most intense. Of interest is the low-level angular momentum at larger radii. As depicted in figure 5, higher angular momentum air is being imparted to the vortex at lower levels. Lewellen et al. (2000) underscored the importance of the low level flow to the overall dynamics of the tornado by introducing a local swirl ratio. The local, or the corner flow, swirl ratio is a property of the surface layer core flow and is uniquely dependent upon the flux of low level angular momentum fluid into the surface layer. As discussed previously, the surface layer inflow affects both the corner region and the core flow. Thus understanding and identifying the changes in the outer flow that contribute to and/or change the momentum flux is paramount to the evolution of the tornado. Moreover, the temporal and spatial variations of the low angular momentum air diverted into the boundary layer and its effects on the evolution of the tornado merit further study. The Mulhall tornado (Lee and Wurman 2005, see their Fig. 4h) exhibited a similar angular momentum distribution.

The derived velocity profiles reveal marked variability in space and in time (Figure 6). Additionally, the variability of the velocity with height in the lowest 100 m does not exhibit the logarithmic decay as specified in this region by Lewellen at al. (1997, 2000). This is not to say that this relationship does not exist; instead, it may be confined to the layer below the lowest elevation scan (~0-20 m). Also noteworthy is the evolution of the velocities in time (Figs. 2 and 4) and the inferred change in vortex structure. Early retrievals indicate a much different vortex structure than at later times. As discussed previously, the swirl ratio is used to diagnose vortex structure and the resultant velocity distribution. While the swirl ratio has historically been idealized as a static parameter, the results presented above further the notion that a time-dependent swirl ratio is a realization in the atmosphere. Thus it is critical to investigate the effects of a changing swirl ratio on vortex dynamics. All of these observations provide a far more complicated picture of the outer boundary conditions than are currently employed in the idealized numerical models of tornadoes, motivating the necessity to use DOW-derived boundary conditions.

4. Future Work

Results from the LES model will be presented at the conference. At present, modifications are being made to the existing code, which will allow for the specified lateral and top boundary conditions derived from the DOW data. Further, the complete radar analysis of the 4D (including time) winds from the Spencer, SD tornado and the Harper, KS tornado will be discussed.

5. Acknowledgements

This work was supported in part by the Purdue Research Foundation Research Grant No. 6904138.

6. References

Davies-Jones, R., R. J. Trapp, and H. B. Bluestein, 2001: Tornadoes and tornadic storms, *Severe Convective Storms, Meteor. Monogr.*, No. 50, Amer. Meteor. Soc., 167-222.

Dowell, D. C., C. R. Alexander, J. M. Wurman, and L. J. Wicker, 2005: Centrifuging of hydrometeors and debris in tornadoes: radar-reflectivity patterns and wind-measurement errors. *Mon. Wea. Rev*., **133**, 1501-1524.

Lee, W.-C., J.-D. Jou, P.-L. Chang, and F. D. Marks, 2000: Tropical cyclone kinematic structure retrieved from single-Doppler radar observations. Part III: Evolution and structure of Typhoon Alex (1987). *Mon. Wea. Rev.*, **128**, 3982-4001.

Lee, W-. C-. and J. Wurman, 2005: Diagnosed three-dimensional axisymmetric structure of the Mulhall tornado on 3 May 1999. *J. Atmos. Sci.*, **62**, 2373-2393.

Lewellen, W.S., 1993: Tornado vortex theory. *The Tornado: Its Structure, Dynamics, Predictions, and Hazards*, Geophys. Monogr., No. 79, Amer. Geophys. Union, 19-39.

Lewellen W. S., D. C. Lewellen, and R. I. Sykes, 1997: Large eddy simulation of a tornado's interaction with the surface. *J. Atmos. Sci.*, **54**, 581-605.

Lewellen, D. C., W. S. Lewellen, and J. Xia, 2000: The influence of a local swirl ratio on tornado intensification near the surface. *J. Atmos. Sci.*, **57**, 527-544.

Moeng, C-.H-., 1984: A large-eddy simulation model for the study of the planetary boundary layer turbulence. **41**, *J. Atmos. Sci.*, 2052-2062.

Skamarock, W. C., J. B. Klemp, J. Dudhia, D. O. Gill, D. M. Barker, W Wang, and J. G. Powers, 2005: A Description of the Advanced Research WRF Version 2, available at http://wrf-model.org/wrfadmin/docs/arw_v2.pdf 100 pp.

7. Figures

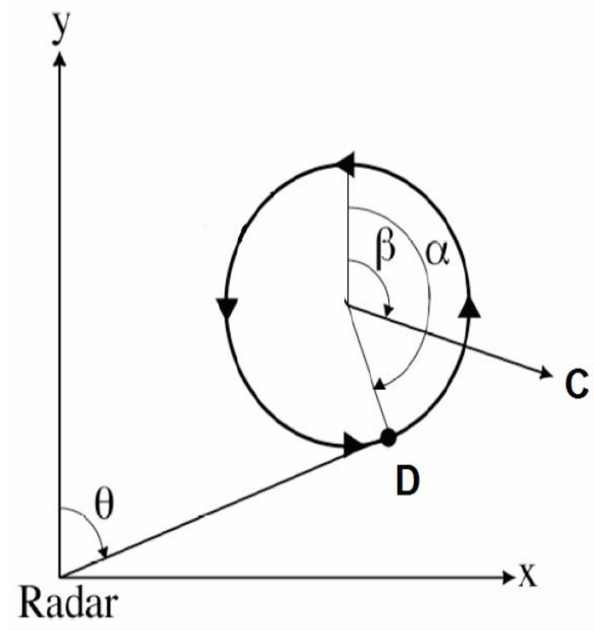

Figure 1: Geometry of the axisymmetric vortex model. Variables described in text.

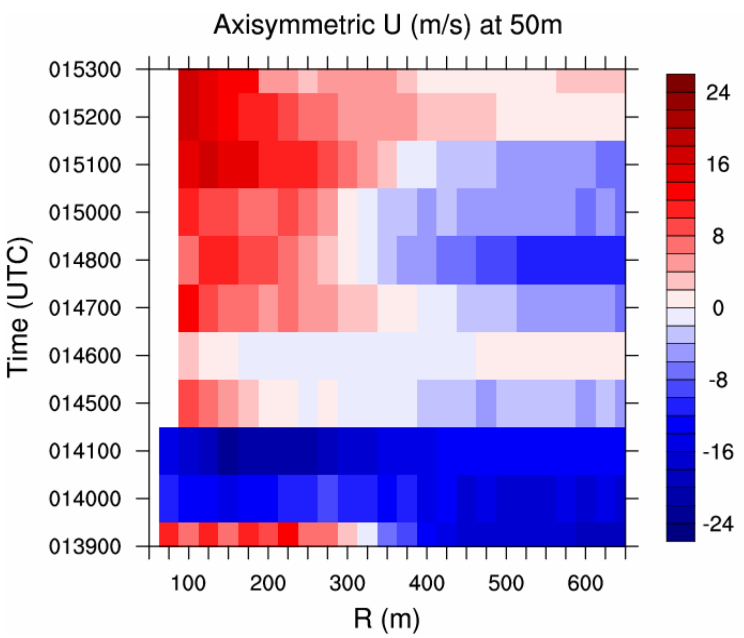

Figure 2: A Hovmoller diagram of the axisymmetric radial velocity (u) as a function of radius and time for z = 50m.

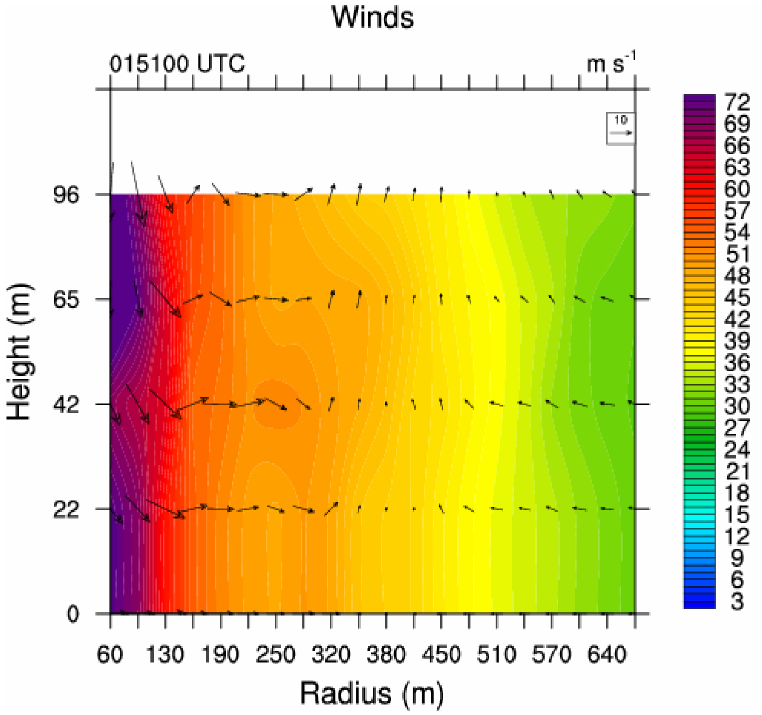

Figure 3: The 3d winds as a function of radius for t = 01:51:00 UTC. Arrows indicate radial/vertical velocities and the contours depict the tangential velocities.

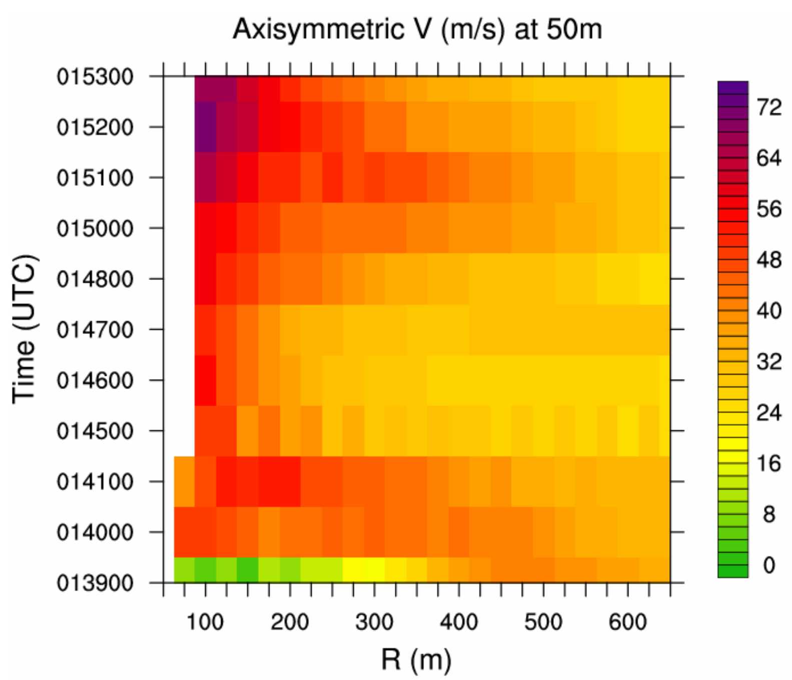

Figure 4: A Hovmoller diagram of the axisymmetric tangential velocity (v) as a function of radius and time for z = 50m.

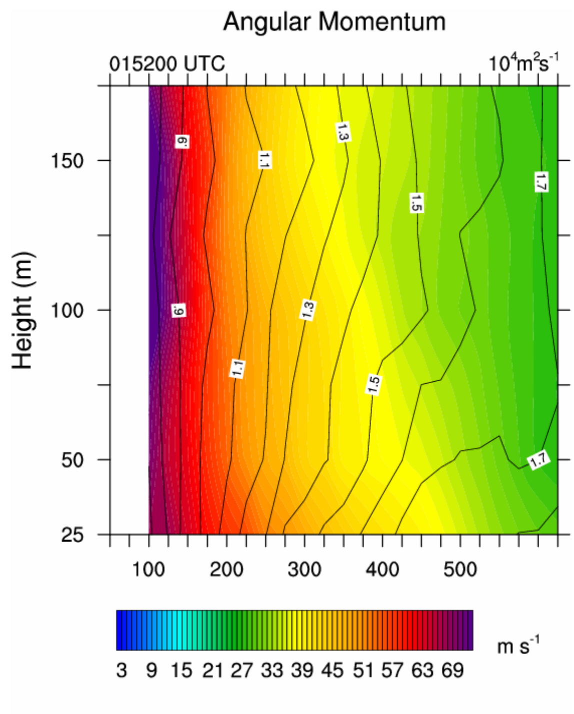

Figure 6: Angular momentum (line contours) overlaid on the axisymmetric tangential winds (colored contours) as a function of height and radius for t = 01:52:00 UTC.

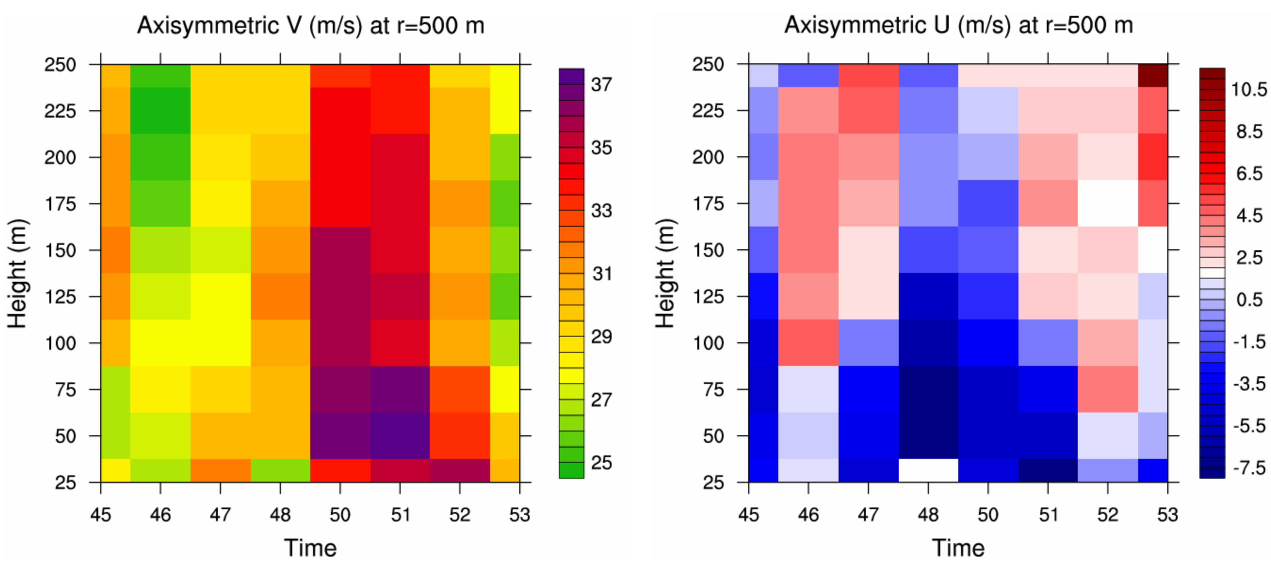

Figure 7: Homoller diagrams of the axisymmetric (a) tangential winds and (b) radial winds as a function of height and time for r =500m. These are representative of the lateral boundary conditions for the LES.